EPJ Web of Conferences **158**, 03013 (2017) DOI: 10.1051/epjconf/201715803013
QFTHEP 2017

Observation and investigation of πK atoms

Valeriy Yazkov[1,⋆] on behalf of the DIRAC collaboration

[1] *D. V. Skobeltsyn Institute of Nuclear Physics, M. V. Lomonosov Moscow State University, Leninskie Gory 1, 119991 Moscow, Russia*

Abstract. There is accurate relation between lifetime of atoms, consisting of pion and kaon, and a difference of S-wave pion kaon scattering length with isospin 1/2 and 3/2: $|a_{1/2} - a_{3/2}|$. This difference is predicted by low energy QCD. Experiment DIRAC at CERN PS detects 349 ± 62 pairs from $K^+\pi^-$ and π^+K^- atoms and make observation of exotic atoms consist of pion and kaons and provides way for measurement of pion-kaon scattering length difference and check of theoretical predictions.

1 Introduction

In 2007, the DIRAC collaboration enlarged the scope of the dimesonic atom investigation by starting to search for the strange pion-kaon (πK) atom. In addition to the ongoing study of $\pi\pi$ atoms, the DIRAC experiment at the CERN proton synchrotron (CERN PS) also collected data, containing a kaon beside a pion in the final state. Using all the data since 2007 and optimizing data handling and analysis, the observation of the πK atom could be achieved for the first time with a significance of more than 5 standard deviations [1].

πK-atom ($A_{\pi K}$) is a hydrogen-like atom consisting of K^+ (K^-) and π^- (π^+) mesons with a Bohr radius of $a_B = 249$ fm, Bohr momentum of $p_B \simeq 0.8$ MeV/c and a ground state Coulomb binding energy of $E_B = 2.9$ keV .

The πK-atom lifetime (ground state 1S), $\tau = \frac{1}{\Gamma}$ is dominated by the annihilation process into $\pi^0 K^0$. There is a relation between the width of $A_{\pi K}$ decay and S-wave πK scattering lengths for isospin 1/2 and 3/2 [2]:

$$\Gamma_{1S,\pi^0K^0} = \frac{1}{\tau_{1S}} = 8\alpha^3\mu^2 p^*(a_0^-)^2(1 + \delta_K). \tag{1}$$

Here S-wave isospin-odd πK scattering length $a_0^- = \frac{1}{3}(a_{1/2} - a_{3/2})$ is defined in pure QCD for the quark masses $m_u = m_d$, α is the fine structure constant, μ is the reduced mass of the $\pi^\pm K^\mp$ system, p^* is the outgoing π^0 momentum in the πK atom system, and δ_K accounts for corrections, due to isospin breaking, at order α and quark mass difference $(m_u - m_d)$.

Chiral Perturbation Theory (ChPT) describes QCD processes at low energies. ChPT in 1-loop approximation predicts S-wave pion-kaon scattering lengths with isospin 1/2 ($a_0^{1/2}$) and 3/2 ($a_0^{3/2}$) to be [3, 4]:

$$a_0^{1/2} = 0.19 \pm 0.2,\ a_0^{3/2} = -0.05 \pm 0.02,\ a_0^{1/2} - a_0^{3/2} = 0.23 \pm 0.01\ . \tag{2}$$

⋆e-mail: valeri.yazkov@cern.ch

ChPT with $L^{(2)}, L^{(4)}, L^{(6)}$ in 2-loop approximation predicts S-wave scattering length difference [5]:

$$a_0^{1/2} - a_0^{3/2} = 0.267\,. \tag{3}$$

Scattering length difference also has been predicted, using Roy-Steiner equations [6]:

$$a_0^{1/2} - a_0^{3/2} = 0.269 \pm 0.015\,. \tag{4}$$

In the framework of lattice QCD, predictions for πK scattering length and their combination a_0^- have been obtained in [7] (Eq. 5), [8] (Eq. 6), [9] (Eq. 7), [10] (Eq. 7):

$$a_0^{1/2} = 0.1725^{+0.0026}_{-0.0157},\ a_0^{3/2} = -0.0574^{+0.0029}_{-0.0060}, \tag{5}$$

$$a_0^{1/2} = 0.183 \pm 0.039,\ a_0^{3/2} = -0.0602 \pm 0.0040, \tag{6}$$

$$a_0^- = \frac{1}{3}(a_0^{1/2} - a_0^{3/2}) = 0.0811 \pm 0.0143\,. \tag{7}$$

$$a_0^- = \frac{1}{3}(a_0^{1/2} - a_0^{3/2}) = 0.0745 \pm 0.0020\,. \tag{8}$$

Prediction of scattering length difference in Eq. (4) provides an estimation of lifetime of $A_{\pi K}$ in ground state:

$$\tau = (3.5 \pm 0.4) \times 10^{-15}\,. \tag{9}$$

There is differences in predictions of $a_0^{1/2} - a_0^{3/2}$ value, obtained in [5, 6] from one side and [7, 10] from another side. It is needed to test predictions experimentally and accuracy of experimental measurement is to be at the level 5%.

The measurement of the S-wave πK scattering lengths would test our understanding of the chiral $SU(3)_L \times SU(3)_R$ symmetry breaking of QCD (u, d and s quarks), while the measurement of $\pi\pi$ scattering lengths checks only the $SU(2)_L \times SU(2)_R$ symmetry breaking (u, d quarks). This is the principal difference between $\pi\pi$ and πK scattering.

Experimental data on the πK low-energy phases are absent. The only experimental pion-kaon scattering length measurement has been done with estimation of πK atom lifetime, using data collected in 2008-2010 with Nickel (Ni) target [11]:

$$|a_0^-|M_\pi = 0.107^{+0.093}_{-0.035}\,. \tag{10}$$

In the present publication experimental data for πK atom investigation, collected in 2008-2010 and data collected in 2007 with Platinum (Pt) target [12] have been analysed with improved description of the setup response.

2 Method of πK atom observation and investigation

A method of investigation for $\pi^+\pi^-$, πK and other atoms, consisted of two oppositely charged mesons, has been proposed in [13]. Pairs of K^+ (K^-) and π^- (π^+) mesons are producing in proton-target interactions. Pairs, which are generated from fragmentation and strong decays ("short-lived" sources), are affected by Coulomb interaction in the final state. Some of them form Coulomb bound states — atoms, other are generated as free pairs ("Coulomb pairs"). Number of produced atoms (N_A) is proportional to a number of "Coulomb pairs" (N_C) with low relative momentum Q in a pair C.M. system: $N_A = K \cdot N_C$. The coefficient K is calculated with an accuracy better than 1% [14].

If at least one meson is generated from long-lived sources (electromagnetically or weakly decaying mesons or baryons: $\eta, \eta', K^0_s, \ldots$), then such pairs ("non-Coulomb pairs") are not affected by interaction in the final states.

After production, $A_{\pi K}$ travel through the target and could to annihilate into $\pi^0 K^0$, or to be ionised due to interaction with the target matter, producing specific "atomic pairs". These pairs have small relative momentum ($Q < 3$ MeV/c) and a number of such pairs n_A could be measured experimentally. Ratio of "atomic pair" number to a number of atom produced is a breakup probability: $P_{\rm br}(\tau) = n_A/N_A = n_A/(K \cdot N_C)$ [15, 16]. In Fig 1 dependence of $A_{\pi K}$ breakup probability is shown for two Ni target are used in experiment DIRAC for pair laboratory momentum range 5.1 ÷ 8.5 GeV/c. Value is averaged, using experimentally measured spectrum of atoms.

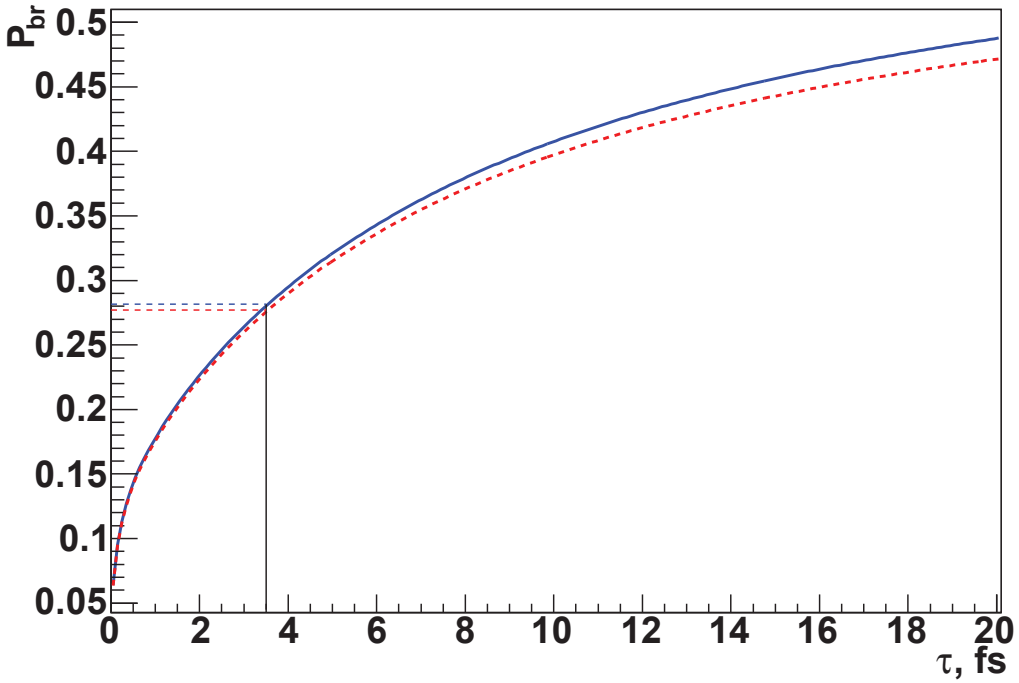

Figure 1. Dependence of the breakup probability $P_{\rm br}$ on $A_{\pi K}$ lifetime for 108μm (solid blue line) and 98μm (dashed red line) Ni targets, and an example how lifetime could be obtained from experimentally measured breakup probability

3 DIRAC setup

DIRAC setup was created to detect $\pi^+\pi^-$ with small relative momenta [17]. In 2004-2006 it has been modified in order to detect both $\pi^+\pi^-$ and πK pairs [18]. New detectors for particle identification have been added: Cherenkov detectors with heavy gas and aerogel for identification of K-mesons among background of pions and protons, correspondingly. Taking into account kinematic of πK "atomic pairs", new detectors cover only internal parts of each arm (see Fig. 2). Aerogel Cherenkov detector is mounted only in positive particle arm, because a flux of antiprotons is small relative to a flux of K^- mesons.

Coordinate resolution of the setup detector provide high resolution over components of relative momentum Q: transverse $\sigma_{Q_X} = \sigma_{Q_Y} = 0.5$ MeV/c and longitudinal $\sigma_{Q_L} = 0.9$ MeV/c (for πK pairs). Time resolution of vertical hodoscope $\sigma_T^{VH} = 100$ ps allows to use time-of-flight technique for suppression of wrongly identified particle pairs.

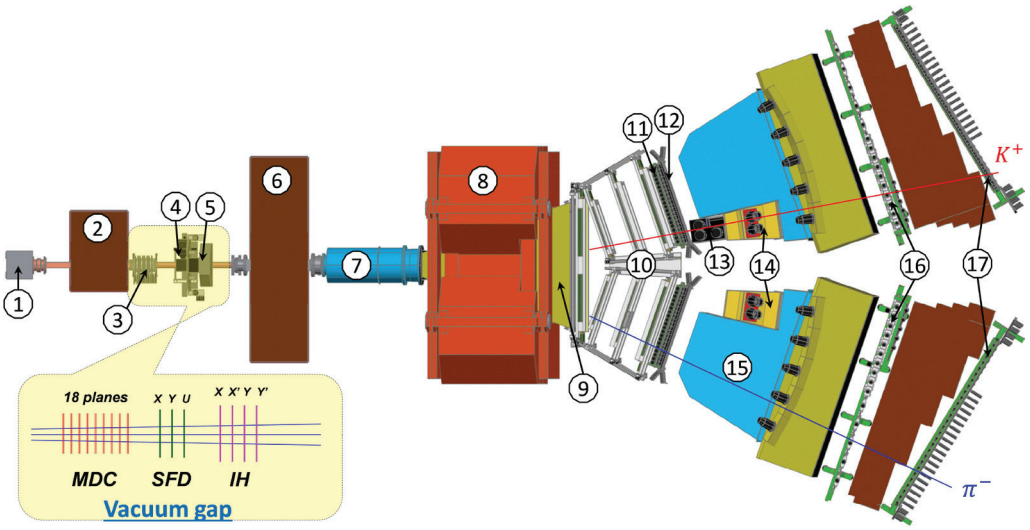

Figure 2. General view of upgraded DIRAC setup (1 – target station; 2 – first shielding; 3 – micro drift chambers (MDC); 4 – scintillating fiber detector (SFD); 5 – ionization hodoscope (IH); 6 – second shielding; 7 – vacuum tube; 8 – spectrometer magnet; 9 – vacuum chamber; 10 – drift chambers (DC); 11 – vertical hodoscope (VH); 12 – horizontal hodoscope (HH); 13 – aerogel cherenkov (ChA); 14 – heavy gas cherenkov (ChF); 15 – nitrogen cherenkov (ChN); 16 – preshower (PSh); 17 – muon detector (Mu).

4 Selection πK events

Analysis procedure selects events which have signals of detectors expected for π^+K^- and $K^+\pi^-$ pairs. Fig. 3(left) presents the distribution of selected events over the difference of the particle production times for K^+ mesons in the range (4.4–4.5) GeV/c. The distribution is fitted by the simulated distribution of $K^+\pi^-$, $\pi^+\pi^-$, pπ^- and accidental pairs. Fig. 3(right) shows the fit for K^+ in the range (5.4–5.5) GeV/c. The contribution of misidentified pairs was estimated and accordingly subtracted [19]. Fraction of non-suppressed background pairs is calculated as function of momentum and used for estimation of systematic uncertainty (see below).

Fig. 4a illustrates the Q_L distribution of potential $K^+\pi^-$ pairs requiring a ChF signal and $Q_T < 4$ MeV/c. The dominant peak on the left side is due to pπ^- pairs from Λ decay. After requesting a ChA signal, the admixture of pπ^- pairs is decreased by a factor of 10 (Fig. 4b). By selecting compatible TOFs between target and VH, background pπ^- and $\pi^+\pi^-$ pairs can be substantially suppressed (Fig. 4c). In the final distribution, the well-defined $K^+\pi^-$ Coulomb peak at $Q_L = 0$ emerges beside the strongly reduced peak from Λ decays at $Q_L = -30$ MeV/c. The Q_L distribution of potential π^+K^- pairs shows a similar behaviour. Applying the ChF and TOF criteria provides a sufficient background

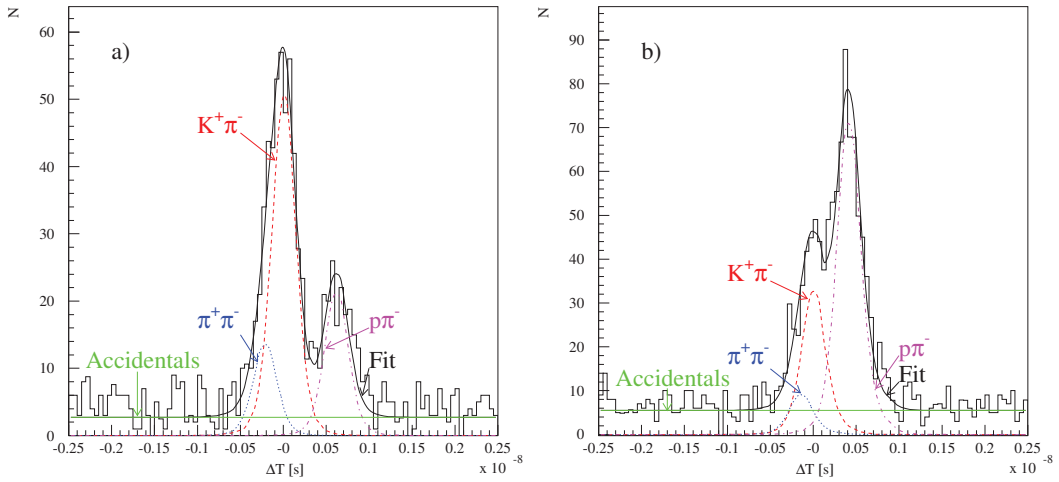

Figure 3. a) difference of particle generation times for events with positively charged particle momenta (4.4 ÷ 4.5) GeV/c. Experimental data (histogram) are fitted by the event sum (black, solid): $K^+\pi^-$ (red, dashed), $\pi^+\pi^-$ (blue, dotted), pπ^- (magenta, dotted-dashed) and accidentals (green, constant). b) similar distributions for events with positively charged particle momenta (5.4 ÷ 5.5) GeV/c.

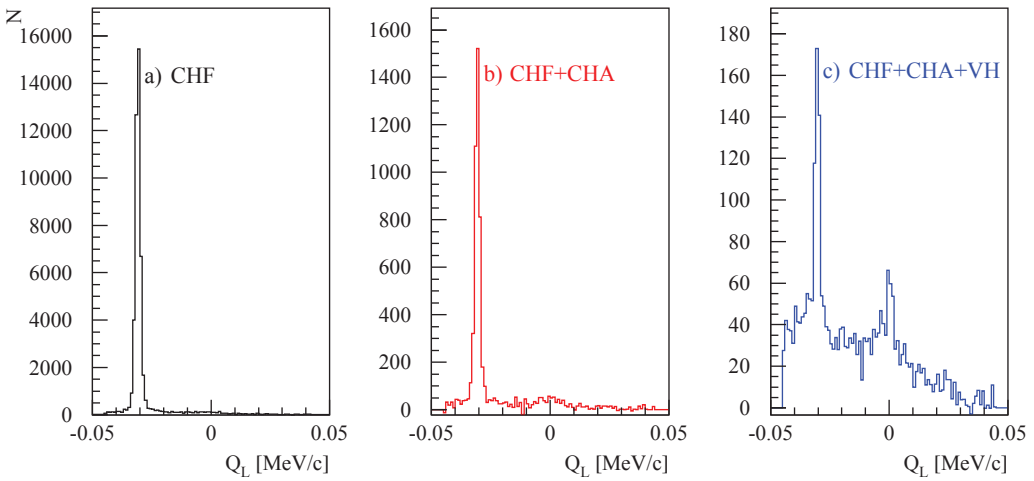

Figure 4. Q_L distribution of $K^+\pi^-$ pairs after applying different criteria (see text).

rejection. Fig. 5 presents the π^+K^- Coulomb peak at $Q_L = 0$ and a second peak from $\bar{\Lambda}$ decays at $Q_L = 30$ MeV/c.

For the final analysis, the DIRAC procedure selects events fulfilling the following criteria:

$$Q_T < 4\text{MeV}/c, |Q_L| < 20\text{MeV}/c\,.$$

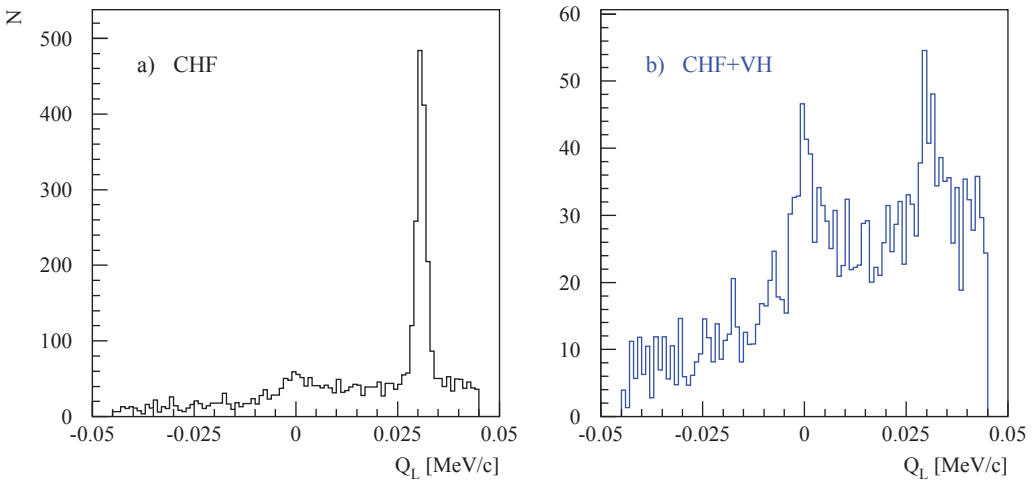

Figure 5. Q_L distribution of π^+K^- pairs after applying different criteria (see text).

Table 1. "Atomic pair" numbers n_A by analysing the 1-dimensional Q and $|Q_L|$ distributions and the 2-dimensional $(|Q_L|, Q_T)$ distribution. Only statistical errors are given.

Analysis	$K^+\pi^-$	π^+K^-	$K^+\pi^-$ and π^+K^-
Q	243 ± 52 (4.7σ)	106 ± 32 (3.3σ)	349 ± 61 (5.7σ)
$\|Q_L\|$	164 ± 79 (2.1σ)	67 ± 47 (1.4σ)	230 ± 92 (2.5σ)
$\|Q_L\|, Q_T$	237 ± 50 (4.7σ)	78 ± 32 (2.5σ)	314 ± 59 (5.3σ)

5 Observation of π^+K^- and $K^+\pi^-$ atoms

Distributions of experimental data over relative momentum Q and its projections Q have been fitted by a sum of simulated distributions of "atomic", "Coulomb" and "non-Coulomb" pairs [20]. Contributions of simulated distributions are free parameters of fit. In order to reproduce distribution of experimental pairs over relative momentum Q and its projections, simulation procedure takes into account resolution and efficiency of the setup detectors, multiplicity of background particles and noise signals, multiple scattering in Pt (run 2007) and Ni (2008-2010) targets, detector planes and partitions.

Fig. 6a presents the experimental and simulated Q distributions of $K^+\pi^-$ pairs for the data obtained from the Pt target and Ni targets. Fig. 7a is for π^+K^- pairs. One observes an excess of events above the sum of "Coulomb" and "non-Coulomb" pairs in the low Q region, where atomic pairs are expected: these excess spectra are shown in Figs. 6b and 7b together with the simulated distribution of atomic pairs. The numbers of atomic pairs, found in the $K^+\pi^-$ and π^+K^- data, are $n_A(K^+\pi^-) = 243 \pm 51$ ($\chi^2/n = 36/37$, n = number of degrees of freedom) and $n_A(\pi^+K^-) = 106 \pm 32$ ($\chi^2/n = 42/37$). Comparing the experimental with the simulated distributions, demonstrates good agreement.

Experimental distribution for sum of π^+K^- and $K^+\pi^-$ data is presented in Fig. 8. Numbers of π^+K^- and $K^+\pi^-$ "atomic pairs" obtained with analysis of one-dimensional distributions over Q and $|Q_L|$ and two-dimensional $(|Q_L|, Q_T)$ distribution are presented in Table 1 (Ni and Pt target together). The best statistical accuracy are achieved by analysis of Q and $(|Q_L|, Q_T)$ distributions. Signal to error ratio is more than 5. The 1-dimensional $|Q_L|$ analysis for all πK data yields $n_A = 230 \pm 92$, which does not contradict the values, obtained in the other two statistically more precise analyses. Compared

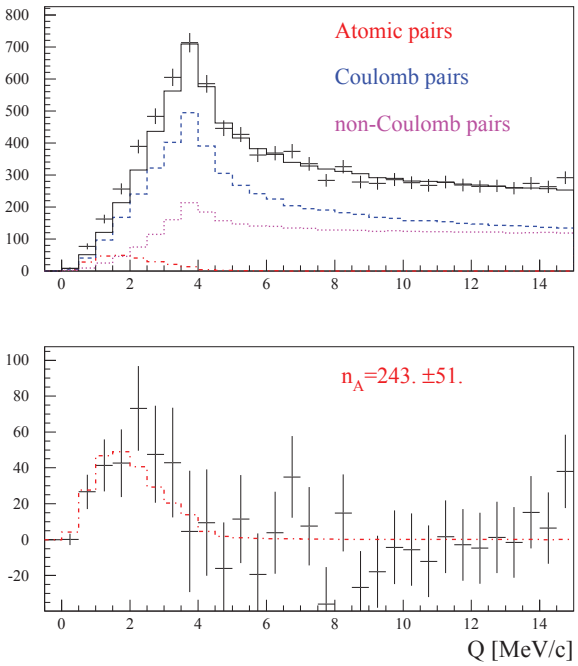

Figure 6. Experimental distribution of $K^+\pi^-$ pairs over Q (upper pictures), shown by points with error bars, is fitted by a sum of simulated distributions of "atomic", "Coulomb" and "non-Coulomb" pairs. The background distribution of free ("Coulomb" and "non-Coulomb") pairs is shown as solid black line. Differences of experimental and background distributions are shown in lower picture together with simulated distributions of "atomic pairs".

to the previous investigation [12], the Pt data was analysed including the upstream detectors. The consequence is a decrease of the statistics, but on the other hand an increase of the Q_T resolution. This better resolution improves the quality of data. Concerning the Ni target, the increase of n_A, compared to [11], is caused by optimizing the time-of-flight criteria, which decreases "atomic pair" losses for the same fraction of background in the final distributions.

The evaluation of the "atomic pair" number n_A is affected by several sources of systematic errors [19, 21]. These uncertainties lead to differences in the shapes of experimental and MC distributions for "atomic", "Coulomb" and to a much lesser extent for "non-Coulomb" pairs. The shape differences induce a bias in the value of the fit parameter n_A, corresponding to a systematic error of the "atomic pair" number. Sources of systematic error and estimation of error values are listed in Table 2.

Taking into account both statistical and systematic errors, the one-dimensional $\pi^{\pm}K^{\mp}$ analysis in Q yields $n_A = 349 \pm 61(stat) \pm 9(syst) = 349 \pm 62(tot)$ "atomic pairs" (5.6 σ) for both combinations of charge and two-dimensional analysis in ($|Q_L|$, Q_T) yields $n_A = 314 \pm 59(stat) \pm 10(syst) = 314 \pm 60(tot)$ "atomic pairs" (5.2 σ). This is the first statistically significant observation of the strange dimesonic πK atom.

6 Measurement of S-wave isospin-odd πK scattering length

Experimentally measured numbers of "atomic pairs" n_A and produced atoms N_A allow (see section 2) to obtain breakup probability $P_{\rm br}$.

Table 3 contains the $P_{\rm br}$ values obtained in the Q and ($|Q_L|$,Q_T) analyses with statistical uncertainties.

Sources of systematic uncertainties of breakup probability are mainly the same like for number of "atomic pairs" (see Table 2). There only one new source - uncertainty in the $P_{\rm br}(\tau)$ relation.

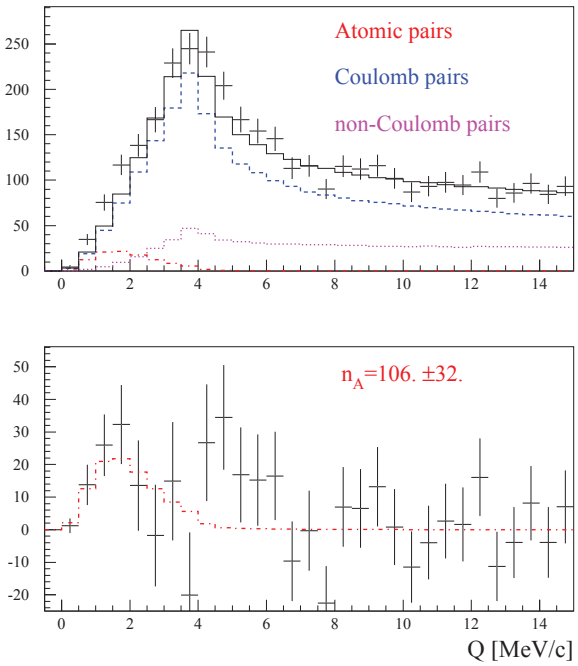

Figure 7. Experimental distribution of π^+K^- pairs analogous to Fig. 6.

Table 2. Estimations of systematic errors, which are induced by different sources, for analysis of data distribution over relative momentum Q, its longitudinal projection $|Q_L|$ and two dimensional distribution over $(|Q_L|, Q_T)$.

Sources of systematic errors	σ^{syst}_{Q}	$\sigma^{syst}_{Q_L}$	$\sigma^{syst}_{\|Q_L\|,Q_T}$
Uncertainty in Λ width correction	0.8	3.0	2.0
Uncertainty of multiple scattering in Ni (Pt) target	4.4	0.7	2.7
Accuracy of SFD simulation	0.2	0.0	0.1
Correction of Coulomb correlation function due to finite size production region	0.0	0.2	0.1
Uncertainty in πK pair laboratory momentum spectrum	3.3	5.4	7.8
Uncertainty in laboratory momentum spectrum of background pairs	6.6	1.6	5.4
Total	8.6	6.4	10.1

Estimations of systematic errors, induced by different sources, are presented in Table 4 for Pt data and Table 5 for Ni data. The total errors were calculated as the quadratic sum. The procedure of the πK atom lifetime estimation described below includes all systematic errors, although their contributions are insignificant compared to the statistical errors.

For estimating the lifetime of $A_{\pi K}$ in the ground state, the maximum likelihood method [22] is applied [23]:

$$L(\tau) = \exp\left(-U^T G^{-1} U/2\right), \tag{11}$$

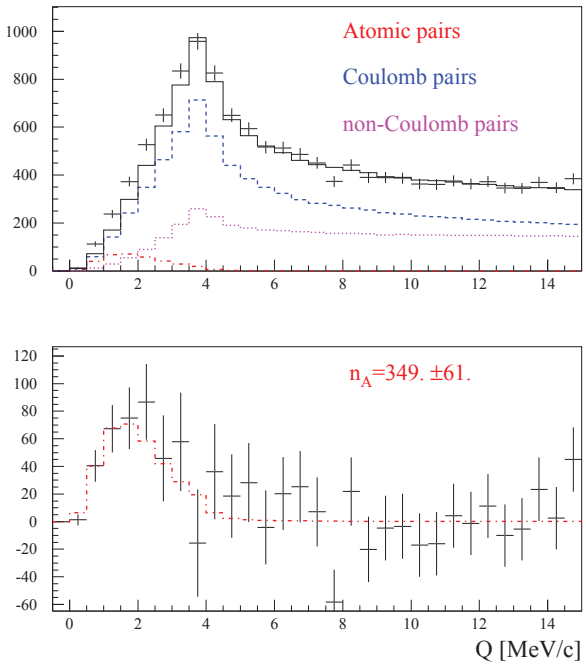

Figure 8. Distribution of π^+K^- and $K^+\pi^-$ pairs over Q (upper pictures), shown by points with error bars, is fitted by a sum of simulated distributions of "atomic" (red dotted-dashed), "Coulomb" (blue dashed) and "non-Coulomb" (magenta dotted) distributions ($\chi^2/n = 41/37$, n = number of degrees of freedom). A sum of background distributions ("Coulomb" and "non-Coulomb") is shown by a solid black line. Differences of experimental and background distributions are shown in lower picture together with simulated distributions of "atomic pairs". Quality of fit, performed in assuption that "atomic pairs" are absent, is worse: $\chi^2/n = 73/38$

Table 3. Experimental $P_{\rm br}$ from Q and $(|Q_L|, Q_T)$ analyses. Only statistical uncertainties are cited.

Data	RUN	Target (μm)	P_{br}^{Q}	$P_{br}^{\lvert Q_L\rvert,Q_T}$
π^+K^-	1	Pt (25.7)	1.2 ± 1.3	0.27 ± 0.56
π^+K^-	2	Ni (98)	0.53 ± 0.39	0.42 ± 0.38
π^+K^-	3	Ni (108)	0.29 ± 0.20	0.33 ± 0.24
π^+K^-	4	Ni (108)	0.33 ± 0.22	0.21 ± 0.20
$K^+\pi^-$	1	Pt (25.7)	1.09 ± 0.52	1.44 ± 0.59
$K^+\pi^-$	2	Ni (98)	0.32 ± 0.20	0.44 ± 0.22
$K^+\pi^-$	3	Ni (108)	0.23 ± 0.16	0.16 ± 0.15
$K^+\pi^-$	4	Ni (108)	0.41 ± 0.17	0.34 ± 0.16
$\pi^+K^-\&K^+\pi^-$	1	Pt, 25.7	1.11 ± 0.48	0.83 ± 0.41

where $U_i = \Pi_i - P_{{\rm br},i}(\tau)$ is a vector of differences between measured Π_i ($P_{\rm br}$ in Table 3) and corresponding theoretical breakup probability $P_{{\rm br},i}(\tau)$ for a data sample i. The error matrix of U, named G, includes statistical (σ_i) as well as systematic uncertainties. Only the term corresponding to the uncertainty in the $P_{\rm br}(\tau)$ relation is considered as correlated between the Ni and Pt data, which is a conservative approach and overestimates this error. The other systematic uncertainties do not exhibit a correlation between the data samples from the Ni and Pt targets. On the other hand, systematic uncertainties of the Ni data samples are correlated. The likelihood functions of the $(|Q_L|, Q_T)$ and Q analyses are shown in Fig. 9.

New estimation of $A_{\pi K}$ lifetime in ground state, based on two-dimensional analysis in $(|Q_L|, Q_T)$:

$$\tau = (3.8^{+3.3}_{-2.0}|_{stat}\,{}^{+1.0}_{-0.6}|_{syst})\,\text{fs} = (3.8^{+3.5}_{-2.1}|_{tot})\,\text{fs}\,, \tag{12}$$

Table 4. Estimated systematic errors of $P_{\rm br}$ for Pt in Q and $(|Q_L|, Q_T)$ analyses.

Source	Q	$(\lvert Q_L\rvert, Q_T)$
Uncertainty in Λ width correction	0.011	0.073
Uncertainty of multiple scattering in the Pt target	0.0087	0.014
Accuracy of SFD simulation	0.	0.
Correction of the Coulomb correlation function on finite size production region	0.0001	0.0002
Uncertainty in πK pair lab. momentum spectrum	0.089	0.25
Uncertainty in the laboratory momentum spectrum of background pairs	0.22	0.21
Uncertainty in the $P_{\rm br}(\tau)$ relation	0.01	0.01
Total	0.24	0.34

Table 5. Estimated systematic errors of $P_{\rm br}$ for Ni in Q and $(|Q_L|, Q_T)$ analyses.

Source	Q	$(\lvert Q_L\rvert, Q_T)$
Uncertainty in Λ width correction	0.0006	0.0006
Uncertainty of multiple scattering in a Ni target	0.0051	0.0036
Accuracy of SFD simulation	0.0002	0.0003
Correction of the Coulomb correlation function on finite size production region	0.0001	0.0000
Uncertainty in πK pair lab. momentum spectrum	0.0052	0.0050
Uncertainty in the laboratory momentum spectrum of background pairs	0.0011	0.0011
Uncertainty in the $P_{\rm br}(\tau)$ relation	0.0055	0.0055
Total	0.0092	0.0084

which corresponds (see Fig. 10(left)) to isospin-odd πK scattering length estimation to be:

$$|a_0^-|M_\pi = 0.087^{+0.043}_{-0.024}|_{tot}\,. \tag{13}$$

Estimation, based on Q analysis:

$$\tau = (5.5^{+4.9}_{-2.8}|_{stat}\ ^{+0.9}_{-0.5}|_{syst})\,\text{fs} = (5.5^{+5.0}_{-2.8}|_{tot})\,\text{fs}\,, \tag{14}$$

provides (see Fig. 10(right)) the following value of the πK scattering length a_0^-:

$$|a_0^-|M_\pi = 0.072^{+0.031}_{-0.020}|_{tot}\,. \tag{15}$$

All theoretical predictions are compatible with the measured value taking into account the experimental precision.

7 Possibility to improve accuracy with experiment at 450 GeV beam

Updated analysis allows to improve accuracy of $|a_0^-|$ measurement from 60% to 40%, but it is still unsufficient for testing predictions of CHPT and LQCD. As shown in [24], the number of πK atoms

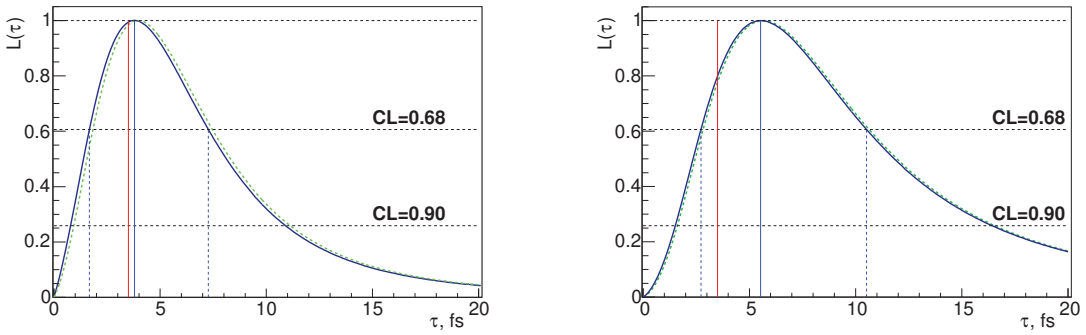

Figure 9. Likelihood functions $L(\tau)$ for $(|Q_L|, Q_T)$ (left) and Q (right) analyses with $Q_T < 4$ MeV/c. The likelihood functions on the basis of both statistical and systematic errors (dashed green line) and on the basis of only statistical error (solid blue line) are presented. The vertical blue lines indicate the best estimate for $\tau_{\rm tot}$ and the corresponding confidence interval. The vertical red line is the theoretical prediction (9).

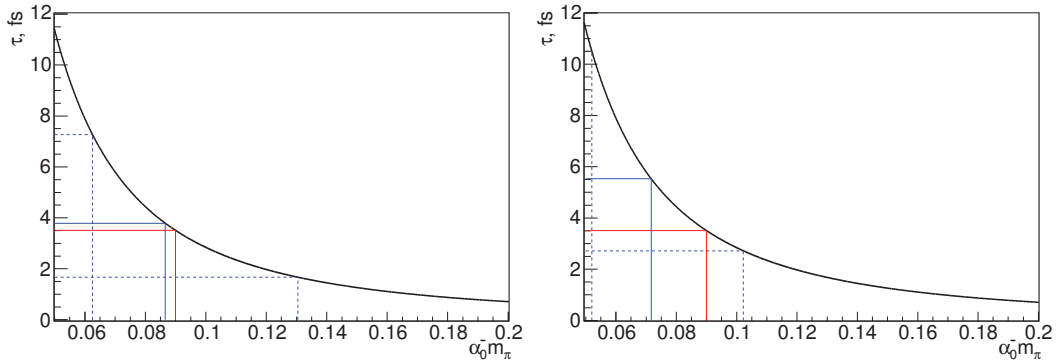

Figure 10. Ground state $A_{\pi K}$ lifetime τ_{1S} versus a_0^-. Experimental results (blue lines) are compared to the theoretical prediction (red lines). $(|Q_L|, Q_T)$ analysis (left) and Q analysis (right).

detected per time unit would be increased by a factor of 30 to 40, if the DIRAC experiment could exploit the CERN SPS 450 GeV/c proton beam. The simulation of atom and charged particle yields and the result of current experimental measurement have been used for estimation of time, which is needed for measurement a_0^- with accuracy 5% [25]. Table 6 presents expected beam time and run time are needed for achievement of this accuracy for present (Ni target only) and modified DIRAC setup. It is seen that experiment at SPS energy allows to measure S-wave pion-kaon scattering length difference with sufficient accuracy for checking theoretical predictions made by ChPT and LQCD.

Expected results of the experiment with 450 GeV beam:

- Expected statistic of πK "atomic pairs": $n_A \approx 13000$.
- Statistical accuracy of πK scattering length difference: $\sim 5\%$.
- Expected systematic error of πK scattering length difference: $\sim 2\%$.
- Expected statistic of $\pi^+\pi^-$ "atomic pairs": $n_A \approx 400000$.
- Statistical accuracy of pion-pion scattering length difference: $\sim 0.7\%$.

Table 6. Estimation of time needed for measurement a_0^- with statistical accuracy $\delta_{a_0^-}$ for present DIRAC setup and beam condition, and for versions Mod1 and Mod2, modified for proton beam energy E_p = 450 GeV and intensity I_B (proton per second). Angle between primary and secondary beams θ_{lab} and solid angle of secondary beam aperture are presented. It is assumed, that at 450 GeV beam the setup would obtain 3000 spills (4.5s) per day.

Setup	E_p GeV	I_b p/s	θ_{lab}	Solid angle *sr*	Beam time s	Run time months	$\delta_{a_0^-}$ %
Present	24	$2.7 \cdot 10^{11}$	5.7	$1.2 \cdot 10^{-3}$	$1.2 \cdot 10^{6}$	14.5	43.
Mod1	450	$1.0 \cdot 10^{11}$	4.0	$0.6 \cdot 10^{-3}$	$5.5 \cdot 10^{6}$	13.6	5.
Mod2	450	$1.0 \cdot 10^{12}$	4.0	$0.6 \cdot 10^{-3}$	$6.5 \cdot 10^{5}$	1.6	5.

- Expected systematic error of pion-pion scattering length difference: $\sim 2\%$.

8 Summary

In the DIRAC experiment at CERN, the dimesonic Coulomb bound states involving strangeness, the $K^+\pi^-$ and π^+K^- atoms, were observed for the first time with reliable statistics. The one-dimensional $\pi^\pm K^\mp$ analysis in Q yields 349 ± 62(*tot*) "atomic pairs" (5.6 σ) for both combinations of charge. Analogously, a two-dimensional analysis in ($|Q_L|, Q_T$) was performed with the result of 314 ± 60(*tot*) "atomic pairs" (5.2 σ).

The breakup probabilities for each atom type and each target are determined. By means of these probabilities, the lifetime of the πK atom in the ground state is evaluated to be:

$$\tau_{\text{tot}} = (5.5^{+5.0}_{-2.8}\big|_{\text{tot}}) \cdot 10^{-15}\text{s}\,,$$

and the S-wave isospin-odd πK scattering length deduced:

$$\left|a_0^-\right| = \frac{1}{3}\left|a_{1/2} - a_{3/2}\right| = (0.072^{+0.031}_{-0.020}\big|_{\text{tot}}) M_\pi^{-1}\,.$$

DIRAC-like experiment at SPS energy provides possibility to check prediction of ChPT and LQCD for pion-kaon scattering lengths with accuracy at the level 5%.

We are grateful to CERN for support and the PS team for the excellent performance of the accelerator. This work was funded by CERN, INFN (Italy), INCITE and MICINN (Spain), IFIN-HH (Romania), the Ministry of Education and Science and RFBR grant 01-02-17756-a (Russia), the Grant-in-Aid from JSPS and Sentanken-grant from Kyoto Sangyo University (Japan).

References

[1] B. Adeva *et al.*, Phys. Rev. Lett. **117**, 112001 (2016)
[2] J. Schweizer, Phys. Lett. B **587**, 33 (2004)
[3] V. Bernard *et al.*, Phys. Rev. D **43**, 2757 (1991)
[4] A. Roessl, Nucl. Phys. B **555**, 507 (1999)
[5] J. Bijnens *et al.*, JHEP **0405**, 036 (2004)
[6] P. Buttiker *et al.*, Eur. Phys. J. C **33**, 409 (2004)
[7] S.R. Beane *et al.*, Phys. Rev. D **77**, 094507 (2008)
[8] C.B. Lang *et al.*, Phys. Rev. D **86**, 054508 (2012)

[9] K. Sasaki *et al.*, Phys. Rev. D **89**, 054502 (2014)
[10] T. Janowski et al., PoS **LATTICE2014** 080 (2015)
[11] B. Adeva *et al.*, Phys. Lett. B **735**, 288 (2014)
[12] B. Adeva *et al.*, Phys. Lett. B **674**, 11 (2009)
[13] L. Nemenov, Sov. J. Nucl. Phys. **41**, 629 (1985)
[14] L. Afanasyev and O. Voskresenskaya, Phys. Lett. B **453**, 302 (1999)
[15] L. Afanasyev and A. Tarasov, Phys. At. Nucl. **59**, 2130 (1996)
[16] M. Zhabitsky, Phys. At. Nucl. **71**, 1040 (2008)
[17] B. Adeva *et al.*, Nucl. Instrum. Methods A **515**, 467 (2003)
[18] B. Adeva *et al.*, Nucl. Instrum. Methods A **839**, 52 (2016)
[19] V. Yazkov and M. Zhabitsky, DN **2013-06** (DN = DIRAC Note), cds.cern.ch/record/1628544
[20] B. Adeva *et al.*, arXiv:1707.02184 [hep-ex]
[21] A. Benelli and V. Yazkov, DN **2016-01**, cds.cern.ch/record/2137645
[22] D. Drijard and M. Zhabitsky, DN **2008-07**, cds.cern.ch/record/1367888
[23] V. Yazkov and M. Zhabitsky, DN **2016-06**, cds.cern.ch/record/2252375
[24] O. Gorchakov and L. Nemenov, J. Phys. G: Nucl. Part. Phys. **43**, 095004 (2016)
[25] V. Yazkov, DN **2016-05**, cds.cern.ch/record/2207227